ARTICLE

# CO$_2$ Sorption Enhanced Steam Reforming of Methane Using Ni/CaO·Ca$_{12}$Al$_{14}$O$_{33}$ Catalysts

**Moisés R. Cesário[1,2], Braúlio S. Barros[3], Yvan Zimmermann[1], Claire Courson[1], Dulce M. A. Melo[2], and Alain Kiennemann[1,*]**

[1]*Laboratoire des Matériaux, Surfaces et Procédés pour la Catlyse—LMSPC, University of Strasbourg, Strasbourg, France*
[2]*Department of Chemistry, Federal University of Rio Grande do Norte, Natal, Brazil*
[3]*School of Science and Technology, Federal University of Rio Grande do Norte, Natal, Brazil*

CO$_2$ sorption enhanced steam reforming of methane (H$_2$O/CH$_4$ ratio = 1 or 3) with Ni/CaO·Ca$_{12}$Al$_{14}$O$_{33}$ catalysts has been studied. Catalysts have been prepared by microwave-assisted self-combustion method. The presence of Ca$_{12}$Al$_{14}$O$_{33}$ favors CaO dispersion and the optimum of activity if excess of CaO is around 75% related to the support. It was demonstrated that with Ni/CaO·Ca$_{12}$Al$_{14}$O$_{33}$ catalysts, the sorption of CO$_2$ on CaO modify the equilibrium of the water gas shift (WGS). Consequently, steam reforming of CH$_4$ is improved both in hydrogen production and in methane conversion even at temperature as low as 650 °C. Time of breakthrough for CO, CO$_2$ and CH$_4$ depends both on excess of CaO and on operating conditions (H$_2$O/CH$_4$ ratio).

**KEYWORDS:**

## 1. INTRODUCTION

The research and development of new sources for "clean" energy, with a significant reduction of the greenhouses gases emission like CO$_2$ are strongly encouraged. Hydrogen is a very attractive fuel for proceeding towards above mentioned goals. Steam methane reforming (SMR) is one of promising routes but represents today and probably for a long time more or less 50% of the sources of hydrogen production.[1] SMR occurs at high temperature ($T \geq$ 800 °C), low pressure (1–5 bar), in presence of a catalyst (often Ni supported on modified alumina) and with an excess of water compared to reaction (1) to facilitate the removal of carbonaceous deposits formed during the methane dissociation. The steam reforming (endothermic reaction) is always accompanied by the exothermic water gas shift reaction (WGSR)[2–5] [reaction (2)]. This allows the improvement of the overall production of hydrogen but leads to undesirable formation of CO$_2$ (at least 3 kg per kg of CH$_4$ consumed).[6] To control CO$_2$ emission, a new interesting process has been described: the reforming optimized by CO$_2$ sorption [reaction (3)]. It associates conventional methane reforming and in situ capture of CO$_2$.[7–9] CO$_2$ regenerated by heating in second reactor then concentrated and purified is directly suitable for a subsequent valorisation in energy products or chemical feedstocks (CH$_4$, CH$_3$OH, DME) by reaction with hydrogen.

$$CH_4 + H_2O \rightarrow CO + 3H_2 \quad \Delta H_{298\,K} = 206.2 \text{ kJ/kmol} \quad (1)$$

$$CO + H_2O \leftrightarrow CO_2 + H_2 \quad \Delta H_{298\,K} = -41.2 \text{ kJ/kmol} \quad (2)$$

$$CaO + CO_2 \leftrightarrow CaCO_3 \quad \Delta H_{298\,K} = -178.2 \text{ kJ/kmol} \quad (3)$$

Different CO$_2$ sorbent materials like zeolites, activated carbons (physisorption), hydrotalcites (adsorption), alkaline or alkaline earth metal oxides have been described in the literature.[10–12] Among alkali and alkali earth metal oxides, calcium oxide is the most used material for several reasons:[13] strong basicity for CO$_2$ sorption, low cost, best balance between equilibrium temperature of CO$_2$ and temperature generally required for SMR. One mole of CO$_2$ reacts stoichiometrically with CaO and the sorption is largely exothermic [reaction (3)]. Taking into account Eqs. (1)–(3), the CO$_2$ sorption partly balances the strong endothermicity of the SMR but also shifts WGSR towards hydrogen formation. However the thermodynamic restrictions of CO$_2$ sorption on CaO require at atmospheric pressure, a temperature slightly lower (650–700 °C) than the usual temperature of SMR[14,15] which is a real challenge. A second challenge is the capacity of CaO to perform CO$_2$ sorption with a high degree of efficiency after several cycles of sorption/desorption. According to the literature on CaO, strongly reduced capacity of CO$_2$ sorption is related to time and number of cycles.[16,17] It is widely accepted that losses of reactivity has a close relation with

the decrease of both surface area and pore volume due to the sintering of the CaO grains.[18] Additionally, the sorption of $CO_2$ on CaO is limited to 70–80% of the theoretical value after 1 h of carbonation with a decrease in the kinetic of the absorption. This is due to the formation on the CaO grains surface of a non porous layer of calcium carbonate which blocks the migration of $CO_2$ to the bulk of the grain (diffusion related problems).

Several strategies are reported in the literature to prevent decrease of efficient sorption cycles and diffusion effects: optimization of calcination conditions,[19] use of an inert support,[20] hydration of the absorbent,[21] reaction with other oxide to obtain new structure. Dolomite (Ca and Mg oxide) showed better results than CaO alone for $CO_2$ sorption after numerous cycles.[22] MgO, for which carbonates are not stable at 600–700 °C, provides a passage allowing access of $CO_2$ inside the CaO–MgO particles. Ni/CaO–MgO has been tested with success for methane and methylnaphthalene steam reforming with an enhancement of the hydrogen production during the $CO_2$ sorption sequence.[6, 23] This result suggests that efficient sorbent could be prepared by mixing CaO with an oxide stable at high temperature and able to form a definite crystalline structure with CaO. $CaAl_2O_4$,[24, 25] $Ca_2Fe_2O_5$[6] or $Ca_{12}Al_{14}O_{33}$[20, 26, 27] have been tested for $CO_2$ sorption. $Ca_{12}Al_{14}O_{33}$ has no $CO_2$ sorption properties but presents a large surface area, provides stable network inhibiting deactivation of CaO by sintering. It appears to be a good candidate to support CaO. However $Ca_{12}Al_{14}O_{33}$ properties (surface area, pore volume) are strongly dependent on the preparation method: solid state reaction,[28] hydration and calcination processes,[29] coprecipitation,[30] mixed-precipitation,[31] mechanical mixing,[32] sol–gel process.[33] $CO_2$ sorption capacity varies significantly with the Ca/Al ratio. As demonstrated for Ni/dolomite[23] and for Ni–Ca based catalysts[34] a bi-functional catalysts for reforming of hydrocarbons and $CO_2$ sorption could be efficient by addition of Ni element to the Ca support.

In this paper we propose the microwaves assisted combustion preparation method[35] for the formation of CaO/$Ca_{12}Al_{14}O_{33}$ with different Ca/Al ratio. Microwave assisted combustion method corresponds to a very low cost, saving time and efficient preparation. After addition of Ni element by impregnation, the bi-functional catalysts were tested in SRM at low temperature (600–700 °C) with $H_2O/CH_4$ ratios 3 and 1. It was expected that $CO_2$ sorption [reaction (3)] would enhance WGSR [reaction (2)] and would favour the activity of methane reforming at low temperatures compatible with the $CO_2$ sorption equilibrium.

## 2. EXPERIMENTAL DETAILS

### 2.1. Sorbents Preparation

The samples with weight ratios of CaO to $Ca_{12}Al_{14}O_{33}$ of 75/25 and 90/10 were prepared by a microwaves assisted self-combustion method using excess of urea in the presence of ammonium nitrate. The precursors reagents were aluminum nitrate [$Al(NO_3)_3 \cdot 9H_2O$–Merck], calcium nitrate [$Ca(NO_3)_2 \cdot 4H_2O$–Merck], urea [$CO(NH_2)_2$–Merck] and ammonium nitrate [$NH_4NO_3$–Merck]. Nitrates are chosen for synthesis because their water solubility, the low temperature to fuse them and their low cost. Urea has the advantage of commercial availability, low cost, high heat generation which is important for the crystallization of desired phases. The ammonium nitrate ensures uniformity of the reaction allowing all the reactants decompose in the same time.

The aluminium, calcium and ammonium nitrates, also called oxidants, were mixed in a Becker type Pyrex with a reducing agent (urea), also known as fuel. After 10 min of stirring on a heating plate, the aqueous suspension was placed in a conventional microwave oven with output power of 800 W and frequency of 2.45 GHz until spontaneous ignition. The resulting powders were then calcined in air at 900 °C for 1.5 h. The powder obtained was sieved to 150 mesh (100 $\mu$m).

As an example, the CA75 sorbent (75%CaO · 25% $Ca_{12}Al_{14}O_{33}$) is prepared as follow: $1.56 \times 10^{-2}$ mol of calcium nitrate, $2.60 \times 10^{-3}$ mol of aluminium nitrate, $6.50 \times 10^{-3}$ mol of urea and $1.25 \times 10^{-1}$ mol of ammonium nitrate were mixed in order to prepare 10 g of the proposed material.

The metal (Ni) impregnation was carried out with a nickel nitrate (> 97% SIGMA ALDRICH—Germany) aqueous solution (0.62 g of salt—5% wt of Ni of the final weight of the CA75 or CA90 sample). The suspension of CA75 or CA90 (2.5 g) in the nitrate nickel solution was kept under stirring at 110 °C by 30 min for solvent evaporation, then the solid was collected, dried overnight at 100 °C and then calcined at 750 °C for 4 h, with a heating rate of 3 °C $min^{-1}$.

For comparison of the absorption capacity, a sample of Ni–CaO was prepared by calcination of calcite at 900 °C for 2 h and then impregnated with a 5% wt Ni (nitrate solution) with further calcination at 750 °C for 4 h with a heating rate of 3 °C $min^{-1}$.

Table I shows the nomenclature of the samples prepared as well as conditions for synthesis.

### 2.2. Sorbents and Catalysts Characterization

The sorbents and impregnated materials were characterized before and after reaction by X-ray diffraction (XRD) using a Bruker D8-Advance diffractometer (Cu K$\alpha$ radiation, with 40 kV and 30 mA). The diffraction powder patterns were obtained in the angular range of 10–90° using step-scanning mode (0.02 °/step) with counting time of 2 s/step.

The nitrogen adsorptions isotherms allow the determination of specific surface area by means of the BET method (Brunauer, Emmett and Teller) on a Micrometrics sorptometer Tri Star 3000. The sorbents and catalysts were degassed at 250 °C overnight before measurement.

**Table I.** Nomenclature and synthesis conditions adopted for each prepared sample.

| Samples-Composition | Precursors | Calcination condition | Nomenclature |
|---|---|---|---|
| 75%CaO·25%Ca$_{12}$Al$_{14}$O$_{33}$ | Al, Ca nitrates | RT to 900 °C/1.5 h 10 °C·min$^{-1}$ | CA75 |
| 90%CaO·10%Ca$_{12}$Al$_{14}$O$_{33}$ | Idem | Idem | CA90 |
| 5%Ni–CaO | Calcite and Ni nitrate | Ni impregnation of CaO then drying and calcination RT to 750 °C/4.0 h 3 °C·min$^{-1}$ | Ni–CaO |
| 5%Ni-CA75 | Ni, Al, Ca nitrates | Ni impregnation of CA75 then drying and calcination RT to 750 °C/4.0 h 3 °C·min$^{-1}$ | Ni-CA75 |
| 5%Ni-CA90 | Idem | Idem as CA75 | Ni-CA90 |

*Notes*: RT: room temperature; $x\% = x$ wt%.

The surface morphology and microstructure of catalysts were identified using a cold field-emission gun scanning electron microscope FEG-SEM (JEOL 6700F).

Temperature-programmed reduction (TPR) was carried out on a Micromeritics AutoChem II to study the reducibility of the catalysts. A mass of 50 mg was placed in a quartz U-tube (6.6 mm internal diameter) and submitted at a total gas flow of 50 ml min$^{-1}$, consisting of a mixture of 90% argon and 10% hydrogen. The heating rate, from room temperature to 900 °C, was 15 °C min$^{-1}$.

For post reaction catalysts the amount of CO$_2$ adsorbed (carbonates formed) was evaluated by temperature programed desorption using the equipment above described for TPR tests. Similar conditions were used but under helium flow.

### 2.3. Catalytic Tests and Ability to Capture of CO$_2$

A TGA Q500 thermal gravimetric analysis equipment was used for the carbonation and calcination experiments. 5–10 mg of sorbents were placed in an aluminium sample cup and heated at 800 °C, under helium slow flow (10 ml min$^{-1}$) for 10 minutes to remove adsorbed water and CO$_2$. Then the temperature was decreased to 650 °C and the valve was switched to a 5 ml min$^{-1}$ CO$_2$ flow (10% in He). The sorption duration was 30 min, with following desorption at 800 °C for 10 min under a 10 ml min$^{-1}$ pure He flow. Multiple cycles, consisting in sorption and desorption steps were repeated to test the ability of sorbents to retain their CO$_2$ sorption capacity.

The experiments of steam reforming of methane enhanced by the CO$_2$ sorption were carried out at 650 °C with duration controlled by the sorption capacity of the samples. The operating conditions for cyclic stepwise sorption-enhanced steam methane reforming over Ni/CaO–Ca$_{12}$Al$_{14}$O$_{33}$ were as follows: feed flow rates under normal conditions: Ar = 26 ml min$^{-1}$ g$_{cat}^{-1}$, CH$_4$ = 1.0 ml min$^{-1}$ g$_{cat}^{-1}$ and H$_2$O = 1.0 ml min$^{-1}$ or 3.0 ml min$^{-1}$ g$_{cat}^{-1}$ (H$_2$O/CH$_4$ = 1 and 3), 2.5 g of catalyst. Water was injected using a syringe pump. The outlet gas was analysed by means of two micro gas chromatographs: the first one, for the separation of CH$_4$, H$_2$ and CO, use a molecular sieve column and the second a HayeSep column for the separation of CH$_4$ and CO$_2$. Before reaction test, the materials were reduced in a 30%H$_2$/Ar flow at 800 °C

for 1 h at a constant heating rate of 10 °C min$^{-1}$. The flow rate of H$_2$ was then cut and the temperature decreased to 650 °C for the addition of water and CH$_4$ in the 1/1 or 3/1 ratios.

In all experiments, catalytic performances were evaluated by CH$_4$ conversion and H$_2$, CO, CO$_2$, CH$_4$ molar fraction calculated as follows:

$$\text{Conversion}(\text{CH}_4)(\%) = \frac{(\text{CH}_4)_{in} - (\text{CH}_4)_{out}}{(\text{CH}_4)_{in}} \cdot 100 \quad (4)$$

$$\text{Molar Fraction } X_n = (AX_n \times f_n) \cdot ((AX_1 \times f_1) + (AX_2 \times f_2)$$
$$+ (AX_3 \times f_3) + (AX_4 \times f_4))^{-1} \quad (5)$$

$X$: product; $A$: peak area; $f$: response factor and $n$: variation 1–4.

## 3. RESULTS AND DISCUSSION

### 3.1. Characterization of Absorbents and Catalysts

#### 3.1.1. XRD

X-ray diffraction patterns of the supports sorbents and Ni catalysts are shown in Figure 1. The phases of cubic structure of NiO (JCPDS File No. 73-1519, with space group Fm-3m), CaO (JCPDS File No. 78-0649, with space group
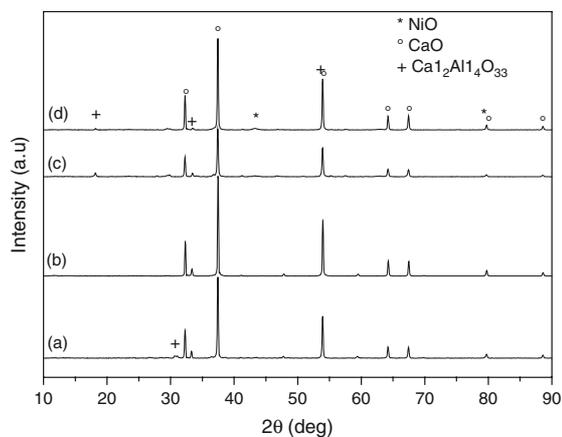


**Fig. 1.** XRD patterns of samples: (a) CA75, (b) CA90, (c) Ni-CA75 and (d) Ni-CA90.

Fm-3m) and Ca$_{12}$Al$_{14}$O$_{33}$ (JCPDS File No. 48-1882, with space group I-43d) were observed.

Preparation method and calcination conditions ensure the selective formation of Ca$_{12}$Al$_{14}$O$_{33}$. No diffraction line corresponding to any other Ca-Al phase such as Ca$_3$Al$_2$O$_6$, CaAl$_2$O$_4$, CaAl$_4$O$_6$ or CaAl$_{12}$O$_{19}$ was observed. After Ni nitrate impregnation followed by calcination neither spinel-type (NiAl$_2$O$_4$) or hydrated structures Ca(OH)$_2$ were observed. The absence of those crystalline phases in the catalysts is important for both the CO$_2$ sorption and the activity in steam reforming of methane.[36]

### 3.1.2. BET

Table II shows the surface areas of the obtained powders. The values of surface area of the two sorbents (supports) are similar but low, those of Ni catalysts are significantly higher. This is due to the hydration process related to Ni impregnation. Previous studies[21] report that the addition of water in the preparation stage of the supports may be responsible for producing regular crystalloid hexagonal Ca(OH)$_2$ which transforms in a porous CaO during calcination at 900 °C leading to an increase in surface area. Such phenomenon occurs in our case during the impregnation of the support with the Ni salt. Difference of BET surface between Ni-CA75 and Ni-CA90 could be due to the amount of CaO effectively present.

### 3.1.3. TPR

The respective TPR profiles of Ni catalysts are shown in Figure 2. Both are similar but the curve of hydrogen consumption of Ni-CA75 is shifted by 40 °C compared to that of Ni-CA90. This corresponds to stronger Ni–CaO or Ni–Ca$_{12}$Al$_{14}$O$_{33}$ interactions for Ni-CA75. For both catalysts, reduction of NiO starts at 420–460 °C and continues until 720 °C which is an indication of different possibilities of metal-support interactions. It can be seen also at 760 °C a small reduction peak probably assigned to the spinel-like structure NiAl$_2$O$_4$. This phase may have been formed during preparation (not detected by XRD) or during TPR.

The diffraction patterns of catalysts after TPR experiments (not given) showed well defined diffraction lines of metallic nickel (JCPDS File No. 87-0712, with space group Fm-3m), CaO and Ca$_{12}$Al$_{14}$O$_{33}$. The average crystallite size of metallic nickel (about 20 nm for both samples)

**Table II.** Specific surface areas of sorbents and catalysts prepared by microwaves assisted combustion method.

| Samples | Calcination temperature/ time | BET surface area before reforming reaction (m$^2$ g$^{-1}$) | Metal content (weight %) |
|---|---|---|---|
| CA75 | 900 °C/1.5 h | 1.2 | – |
| CA90 | 900 °C/1.5 h | 1.3 | – |
| Ni-CA75 | 750 °C/4.0 h | 11.5 | 3.55 |
| Ni-CA90 | 750 °C/4.0 h | 6.4 | 3.85 |
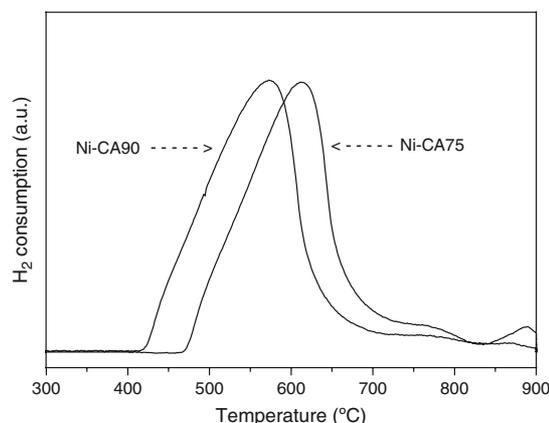


**Fig. 2.** Temperature-programmed reduction (TPR) profiles of the catalysts: Ni-CA75 and Ni-CA90.

was calculated from broadening of the main diffraction rays using the Scherrer equation. The amount of consumed hydrogen during TPR indicates that all the Ni oxides have been reduced to Ni.

### 3.2. CO$_2$ Sorption Experimental Results

Figure 3 shows the CO$_2$ sorption capacity of the support-sorbents and catalysts after five cycles of carbonation/calcination cycles. Clearly, the presence of Ca$_{12}$Al$_{14}$O$_{33}$ enhances and stabilizes the absorption capacity (Ni–CaO compared to Ni-Ca75 and Ni-Ca90). This is in accordance to a better dispersion of the calcium aluminate phase between the CaO grains preventing agglomeration either of CaO responsible of CO$_2$ capture
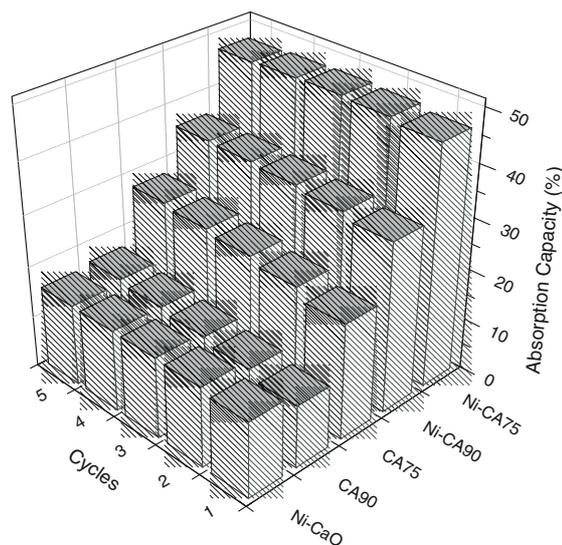


**Fig. 3.** Comparison of cyclic sorption CO$_2$ capacity on the supports and catalysts: Ni–CaO, CA75, CA90, Ni-CA75 and Ni-CA90 (CO$_2$ sorption: 650 °C, 30 min, 10% CO$_2$/He; desorption: 800 °C, 10 min, 100% He).
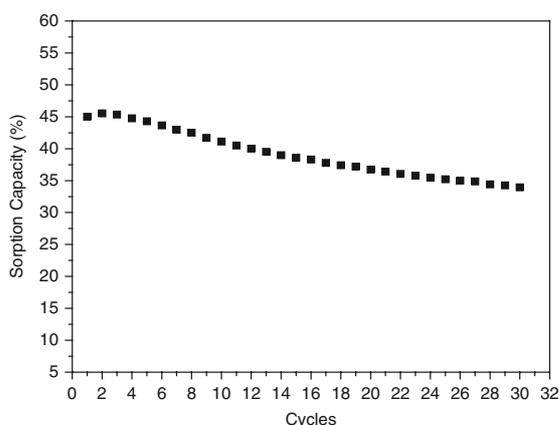
**Fig. 4.** CO₂ sorption capacity of Ni-CA75 during 30 cycles of sorption/desorption. (CO₂ sorption: 650 °C, 30 min, 10% CO₂/He; desorption: 800 °C, 10 min, 100% He).
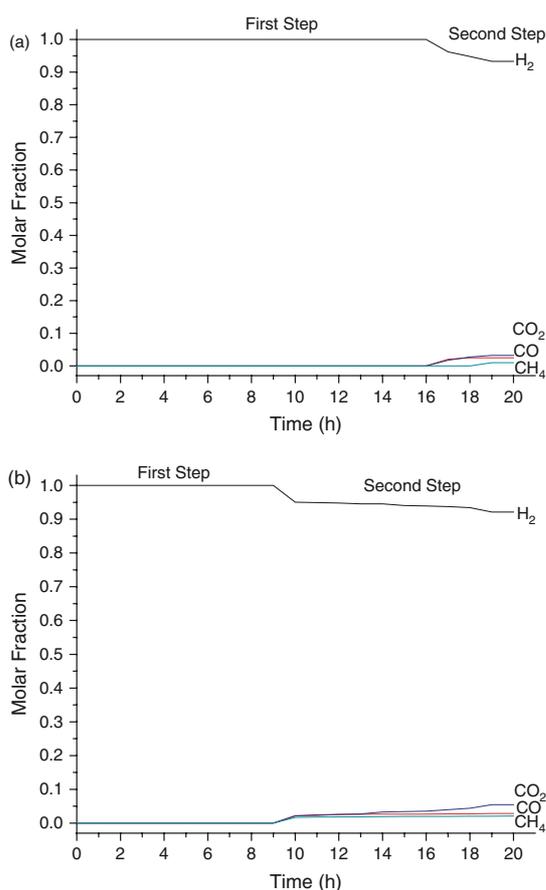


**Fig. 5.** Simultaneous methane steam reforming and CO₂ capture: molar fraction of methane and products versus time (a) Ni-CA75; (b) Ni-CA90. Reaction conditions: Flow rate (Ar = 26 ml · min⁻¹, CH₄ = 1.0 ml · min⁻¹, H₂O = 1.0 ml · min⁻¹); mass of catalyst = 2.5 g, molar H₂O/CH₄ ratio = 1, temperature 650 °C.
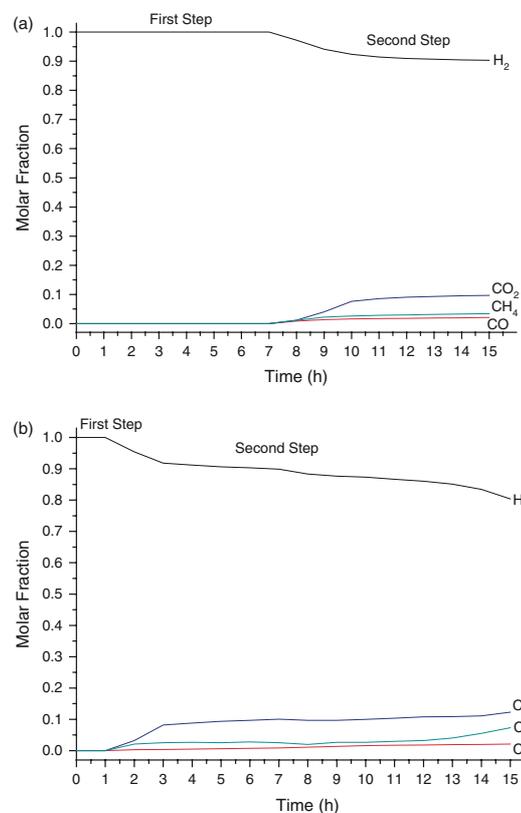


**Fig. 6.** Simultaneous methane steam reforming and CO₂ capture: molar fraction of methane and products versus time (a) Ni-CA75; (b) Ni-CA90. Reaction conditions: Flow rate (Ar = 26 ml · min⁻¹, CH₄ = 1.0 ml · min⁻¹, H₂O = 3.0 ml · min⁻¹); mass of catalyst = 2.5 g, molar H₂O/CH₄ ratio = 3, temperature 650 °C.

or of CaCO₃. Previous studies already showed the stability of CaO in repeated absorption-desorption cycles due to the use of Ca₁₂Al₁₄O₃₃ in the matrix.[20, 29]

The presence of Ni also improves the sorption properties (CA-75 and CA-90 compared to Ni-Ca75 and Ni-Ca90). This is related to the increase in BET surface area after Ni salt impregnation. Martavaltzi et al.[37] also pointed out that the presence of NiO helped to optimize the CO₂ sorption capacity.

The absorption capacity was computed as a fraction of the total carbonation for free CaO. After five sorption/calcination cycles the samples Ni–CaO, CA90, CA75, Ni-CA90 and Ni-CA75 reached values of 15.8, 16.5, 27.4, 35.6 and 47.2%, respectively. The Ca₁₂Al₁₄O₃₃ had a null CO₂ sorption capacity (not shown).

It can be observed that during the five cycles both samples CA75 and CA90 showed a slight increase in sorption capacity, however, the absorption capacity of the CA75 is higher than that of CA90. The CA90 sorbent exhibits a lower performance due the formation of a CaCO₃ layer which prevents the absorption of CO₂ on CaO. Ni-CA90

**ARTICLE**
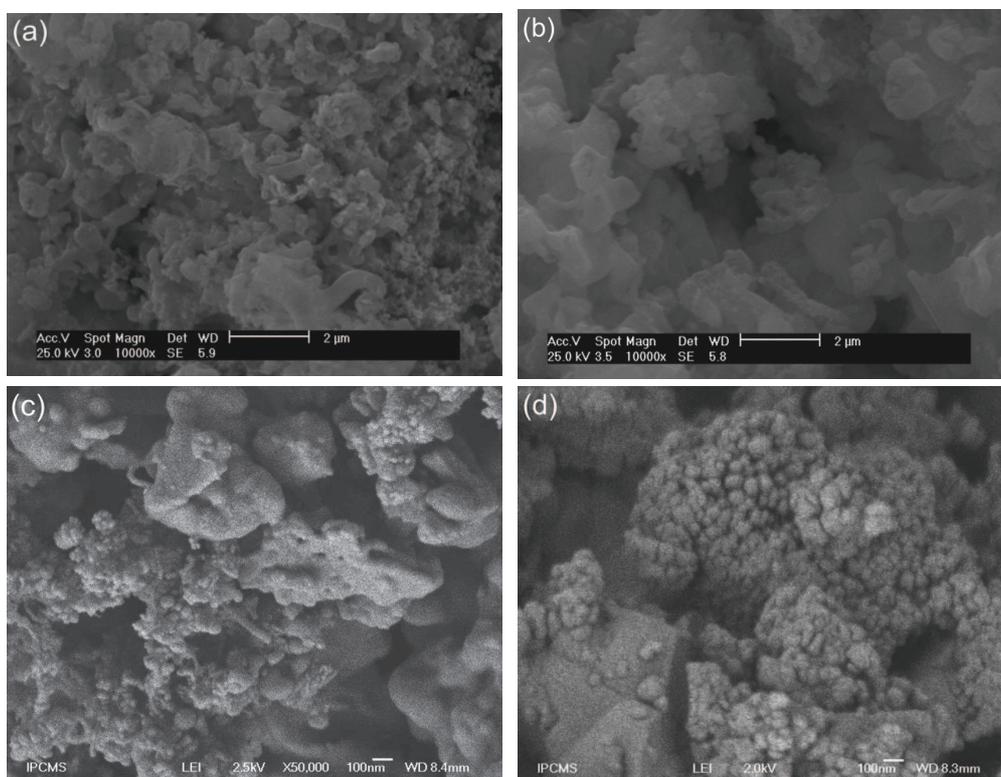
**Fig. 7.** SEM micrographs of: (a) Ni-CA75 and (b) Ni-CA90 before test (c) Ni-CA75 and (d) Ni-CA90 after tests of $CO_2$ sorption-enhanced steam methane reforming (ratio $H_2O/CH_4 = 3$).

catalyst also showed a slight increase in sorption capacity and a lower value in sorption capacity than Ni-CA75 for the same reason.

Sorption capacity of Ni-CA75 was tested to a larger number of absorption/desorption cycles in order to verify the stability of the absorption capacity for a long period. Figure 4 shows the performance along 30 cycles of carbonation/calcination.

We observe a decay of the sorption capacity but after approximately 24 cycles, absorption stabilizes and reaches 35% after 30 cycles (47.2% after 5 cycles). With the same ratio CaO to Ca$_{12}$Al$_{14}$O$_{33}$ but prepared by a process involving hydration followed by calcination, Martavaltzi et al.[37] reported for NiO–CaO·Ca$_{12}$Al$_{14}$O$_{33}$ a similar $CO_2$ absorption capacity of 31%.

### 3.3. Activity for Sorption Enhanced Steam Reforming of Methane

Figures 5 and 6 show performances of the catalysts in SMR optimized by sorption for a $H_2O/CH_4$ ratio equal to 1 and 3, respectively.

As it can be clearly noted the process here reported is divided in two steps, in which the total time of the first one depends of the characteristics of the catalyst as well as of the operating conditions (in our case $H_2O/CH_4$ ratio).

With $H_2O/CH_4$ ratio = 1, Ni-CA75 and Ni-CA90 showed a breakthrough time for $CO_2$ equal to 16 and 9 h, respectively. This can be justified by a greater sorption capacity of Ni-CA75 as shown in Figure 3. With more water ($H_2O/CH_4$ ratio = 3) the length of the breakthrough time decreases significantly to 7 h and 1.5 h, respectively but Ni-CA75 has always the best performances. With lower CaO excess (48 and 65%) the methane conversion is similar but the breakthrough time is reduced (2 and 4 h respectively), compared to 75% CaO excess (curves not given). Due to the greater amount of water, competition between water and $CO_2$ occurs with the formation of carbonates and hydroxides. Thus, smaller amount of CaO are available to absorb $CO_2$ and consequently, breakthrough time is shorter.

In the first step, only the hydrogen is produced with total conversion of $CH_4$. All CO produced during steam reforming is oxidized into $CO_2$ which is totally absorbed throughout. The activation of the three reactions of the process (reforming reactions, water gas shift and carbonation) occurs. The duration of this period depends on the properties of the sorbent, (absorption capacity and absorption kinetics) as well as operating conditions.[38]

Then a sudden drop in the formation of hydrogen associated with the increase in CO, $CO_2$ and methane is observed
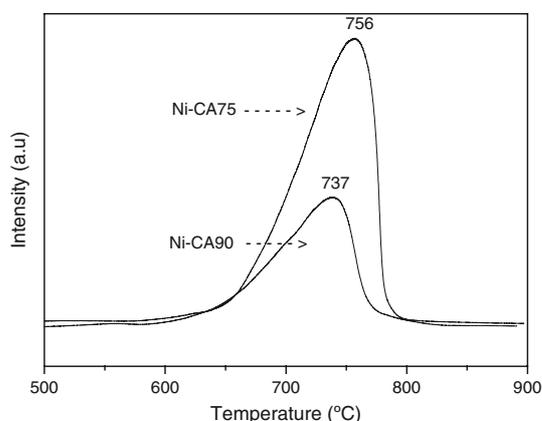
**Fig. 8.** Temperature-programmed desorption (TPD) profiles of $CO_2$ for Ni-CA75 and Ni-CA90 after tests of $CO_2$ sorption-enhanced steam methane reforming (ratio $H_2O/CH_4 = 3$).

(step 2). This exactly corresponds to the end of the CaO carbonation to calcium carbonate (confirmed by XRD). Therefore, $CO_2$ absorption is no more possible, the water gas shift and steam reforming reactions are not shifted to the right (reactions 1 and 2) and methane conversion decreases as shown in Figures 5 and 6. Then hydrogen, CO and $CO_2$ formation and methane conversion remain constant. Results seems to point out that the activity decay is mainly due not to the catalysts deactivation but to the end of $CO_2$ absorption. Moreover, no carbon residue (main cause of deactivation in steam reforming) was observed by SEM or by temperature programmed oxidation (TPO).

### 3.4. SEM, TPD After Tests of Sorption-Enhanced Steam Reforming of Methane

Figure 7 shows the SEM micrographs of the catalysts before and after tests of $CO_2$ sorption enhanced SMR. Before catalytic tests both samples exhibited a similar microstructure with large porous agglomerates composed of fine particles. SEM micrographs obtained after the catalytic tests evidence a typical microstructure of calcium carbonate which is formed during the carbonation reaction, but no traces of residual carbon.

The profiles of temperature-programmed desorption of $CO_2$ are given in Figure 8. Maximum of $CO_2$ desorption occurs at 736–756 °C corresponding to the decomposition of calcium carbonates.[14] Ni-CA75 catalyst showed a more intense peak of $CO_2$ ($\sim 0.1$ mol released $g_{cat}^{-1}$) compared to Ni-CA90 (0.02 mol) after 15h of catalytic activity. This result confirms that $CO_2$ capture for Ni-CA75 was more effective than for Ni-CA90 as firstly seen with the results of sorption and XRD.

### 4. CONCLUSIONS

A new method for the preparation of $CaO \cdot Ca_{12}Al_{14}O_{33}$ support materials for Ni catalysts by microwave-assisted

self-combustion was developed. The formation of $Ca_{12}Al_{14}O_{33}$ phase by a reaction between CaO and alumina allows better dispersion of the CaO excess, which promotes $CO_2$ sorption. There is an optimum for this excess and the best compromise corresponds to an excess of 75% of CaO. Addition of Ni by wet impregnation improves the surface area and $CO_2$ sorption. The Ni catalysts have been tested in catalytic steam reforming of methane with simultaneous absorption of $CO_2$. The CaO carbonation shifts the equilibrium of the water gas shift and improves both productivity of SMR and selectivity to hydrogen after total carbonation of the CaO, conversion of methane decreases and both CO and $CO_2$ appear in the gas phase. Time of breakthrough for CO, $CO_2$ and $CH_4$ depends both on excess of CaO with an optimum and on operating conditions ($H_2O/CH_4$ ratio). The Ni-CA75 catalyst was found the most efficient and performed well even at an unusually low temperature (650 °C) for SMR.

### References and Notes

1. N. H. Florin and A. T. Harris, *Chem. Eng. Sci.* 63, 287 (**2008**).
2. A. Boyano, A. M. Blanco-Marigorta, T. Morosuk, and G. Tsatsaronis, *Energy* 36, 2202 (**2011**).
3. Y. Matsumura, and T. Nakamori, *Appl. Catal., A* 258, 107 (**2004**).
4. E. Simsek, A. K. Avci, and Z. I. Önsan, *Catal. Today* 178, 157 (**2011**).
5. U. Izquierdo, V. L. Barrio, J. F. Cambra, J. Requies, M. B. Güemez, P. L. Arias, G. Kolb, R. Zapf, A. M. Gutiérrez, and J. R. Arraibi, *Int. J. Hydrogen Energy* 37, 7026 (**2012**).
6. L. Di Felice, C. Courson, P. U. Foscolo, and A. Kiennemann, *Int. J. Hydrogen Energy* 36, 5296 (**2011**).
7. K. Johnsen, H. J. Ryu, J. R. Grace, and C. J. Limb, *Chem. Eng. Sci.* 61, 1195 (**2006**).
8. J. A. Satrio, B. H. Shanks, and T. D. Wheelock, *Energy Fuels* 21, 322 (**2007**).
9. D. P. Harrison, *Ind. Eng. Chem. Res.* 47, 6486 (**2008**).
10. S. Sircar, T. C. Golden, and M. B. Rao, *Carbon* 34, 1 (**1996**).
11. E. L. G. Oliveira, C. A. Grande, and A. E. Rodrigues, *Sep. Purif. Technol.* 62, 137 (**2008**).
12. Z. Yong, V. Mata, and A. E. Rodrigues, *Ind. Eng. Chem. Res.* 40, 204 (**2001**).
13. N. H. Florin and A. T. Harris, *Energy Fuels* 22, 2734 (**2008**).
14. G. F. Labiano, A. Abad, L. F. De Diego, P. Gayan, and J. Adanez, *Chem. Eng. Sci.* 57, 2381 (**2002**).
15. I. Barin, Thermochemical Data of Pure Substances, Wiley Publisher, Weinheim (**1989**), Vols. 1–2.
16. J. C. Abanades and D. Alvarez, *Energy Fuels* 17, 308 (**2003**).
17. G. P. Curran, C. E. Fink, and E. Gorin, CO₂ Acceptor Gasification Process, Fuel Gasification, edited by F. C Schora, American Chemical Society Publisher, Washington, DC (**1966**), pp. 141.
18. R. Barker, *J. Appl. Chem. Biotechnol.* 24, 221 (**1974**).
19. A. Silaban and D. P. Harrison, *Chem. Eng. Commun.* 137, 177 (**1995**).
20. C. S. Martavaltzi and A. A. Lemonidou, *Microporous Mesoporous Mater.* 110, 119 (**2008**).
21. C. S. Martavaltzi and A. A. Lemonidou, *Ind. Eng. Chem. Res.* 47, 9537 (**2008**).
22. A. Silaban, M. Narcida, and D. P. Harrison, *Chem. Eng. Commun.* 146, 149 (**1996**).
23. L. Di Felice, C. Courson, N. Jand, K. Gallucci, P. U. Foscolo, and A. Kiennemann, *Chem. Eng. J.* 154, 375 (**2009**).
24. Z. Li, N. Cai, and Y. Huang, *Ind. Eng. Chem. Res.* 45, 1911 (**2006**).

ARTICLE

25. Y. Li, R. Sun, C. Liu, H. Liu, and C. Lu, *Int. J. Greenhouse Gas Control* 9, 117 (**2012**).

26. Z. Zhou, Y. Qi, M. Xi, Z. Cheng, and W. Yuan, *Chem. Eng. Sci.* 74, 172 (**2012**).

27. J. Mastin, A. Aranda, and J. Meyer, *Energy Procedia* 4, 1184 (**2011**).

28. C. Li, D. Hirabayashi, and K. Suzuki, *Appl. Catal., B* 88, 351 (**2009**).

29. Z.-S. Li, N.-S. Cai, Y.-Y. Huang, and H.-J. Han, *Energy Fuels* 19, 1447 (**2005**).

30. H. Chen and C. Zhao, *Chem. Eng. J.* 171, 197 (**2011**).

31. N. Florin and P. Fennell, *Energy Procedia* 4, 830 (**2011**).

32. V. Manovic and E. J. Anthony, *Environ. Sci. Technol.* 43, 7117 (**2009**).

33. M. Broda, A. M. Kierzkowska, and C. R. Müller, *Environ. Sci. Technol.* 46, 10849 (**2012**).

34. M. Broda, A. M. Kierzkowska, D. Baudouin, Q. Imtiaz, C. Copéret, and C. R. Müller, *ACS Catal.* 2, 1635 (**2012**).

35. B. S. Barros, D. M. A. Melo, S. Libs, and A. Kiennemann, *Appl. Catal., A* 378, 69 (**2010**).

36. A. A. Lemonidou and I. A. Vasalos, *Appl. Catal., A.* 228, 227 (**2002**).

37. C. S. Martavaltzi and A. A. Lemonidou, *Chem. Eng. Sci.* 65, 4134 (**2010**).

38. C. S. Martavaltzi, E. P. Pampaka, E. S. Korkakaki, and A. A. Lemonidou, *Energy Fuels* 24, 2589 (**2010**).

ARTICLE